DATA REDUCTION AND THERMAL PRODUCT DETERMINATION FOR SINGLE AND MULTI-LAYERED SUBSTRATES THIN-FILM GAUGES

N. Billiard, V. Iliopoulou, F. Ferrara, R. Dénos
Von Karman Institute for Fluid Dynamics
Turbomachinery & Propulsion Department
Chaussée de Waterloo, 72
1640 Rhode Saint Genèse
(contact: denos@vki.ac.be)

ABSTRACT

Single and two-layered substrate thin film gages allow the determination of wall heat flux when testing in short duration blowdown wind tunnel.

A numerical data reduction technique is proposed and validated to solve the unsteady heat conduction equation with multiple layer substrates.

Then, different methods for the determination of the thermal properties of single or two-layered substrates are applied and compared. Finally, the numerical technique and the determined thermal properties are used to perform measurements on a stator blade using two-layered thin film gauges.

INTRODUCTION

A key parameter to increase the efficiency of a gas turbine is the augmentation of the turbine inlet temperature. The intensive cooling of high-pressure turbine stages allows operating with gas temperature above the melting temperature of the super-alloys that constitute the vanes and the blades. The optimal design of a cooling scheme requires the knowledge of the heat exchange coefficient around the considered airfoil. Not only the mean levels of heat fluxes should be known but also the variations due to blade passage events that constitute a major contribution to high cycle fatigue.

This contribution focuses on data reduction techniques and thermal product determination methods that intend to improve the accuracy of heat transfer measurements performed in blowdown wind tunnels using single or two-layered thin-film gauges.

The single-layered thin-film gauges used at VKI consist of a platinum thin-film fired onto a MACOR machinable glass ceramic substrate. These gauges have been used on vanes (Arts & al., 1990) or as inserts fitted into metallic rotor blades (Dénos, 1996).

The multi-layer gauge technique was intensively developed at the University of Oxford (Doorly & Oldfield, 1986). In this case, the sensing element is deposited on a thin insulating layer, such as an enamel coating or a polyamide sheet bonded with double-sided adhesive. They provide a faster and more flexible implementation than the ceramic inserts but their data reduction is more complex due to the fact that the thermal properties of the successive layers must be known. In this paper, Nickel thin-film gauges deposited onto a Upilex sheet are investigated.

First, the operating principle of single or multi-layered thin-film gauges is reminded. Existing analytical solutions are presented and commented. Then, a numerical solution based on the resolution of the unsteady conduction equation using a Crank-Nicholson scheme is introduced and validated. It can perform the data reduction for both single and multi-layered gauges. Several techniques are tested for the determination of the thermal product of substrates and applied on various materials. Finally, the determined thermal properties and the data reduction technique are used to process experimental data acquired on a turbine stator tested in a one and a half stage environment in the VKI CT3 compression tube facility. Both time-averaged and time-resolved (due to rotor blade passing events) data are processed.

NOMENCLATURE

Roman

C	specific heat at constant pressure [J/kg K]
D	diameter of the nozzle [m]
Nu	Nusselt number
Re	Reynolds number
T	temperature [K]
U	velocity of the jet [m/s]
a	convolution coefficient
c	blade chord [m]
d	thickness of the layer [m]
h	convective heat transfer coefficient [W/ m^2K]
k	thermal conductivity [W/m K]
p	Laplace domain variable
$\dot{q}$	heat flux [W/m^2]
t	time [s]
x	axis perpendicular to the gauges surface [m]

Greek

α thermal diffusivity [m^2/s]

ν kinematic viscosity [m^2/s]

ρ density [kg/m^3]

Subscripts

0 initial condition

i index for the substrate layers

j index for space

m index for time

OPERATING PRINCIPLE

The determination of the heat transfer coefficient h by convection requires the knowledge of 1) the gas temperature, the 2) wall temperature and 3) the heat flux at the wall :

$$h = \frac{\dot{q}_{wall}(t)}{\left(T_{gas} - T_{wall}(t)\right)} \qquad (1)$$

1) The gas temperature is generally measured with a thermocouple.

2) The surface temperature is monitored by the thin-film gauge. It consists of a small and thin strip of a highly conductive material painted onto an insulating substrate. The sensing element of the thin-film acts as a variable resistance thermometer. A high thermal sensitivity is desired (e.g. nickel or platinum). The change of resistance of the sensing element is monitored in a Wheatstone bridge. A controlled temperature oil bath calibration allows determining the linear relationship that links the change of resistance to the change of temperature. The resistive element is connected to wires with gold or copper paths of negligible resistance.

3) The heat flux is derived from the wall surface temperature history during a blowdown test: hot gas is suddenly released on the cold instrumented test body and the surface temperature rises as a function of time. The higher the heat flux, the faster the temperature rises. If the thermal properties of the substrate are known and if the thickness of the substrate is such that at a given depth x, the temperature can be considered as constant during the short testing time (semi-infinite substrate hypothesis), the 1D unsteady conduction equation can be solved with the wall temperature history and the constant (initial) temperature at depth x as boundary conditions.

The sensing element of the gauge is so thin and conductive that it can be neglected in the conduction phenomenon. The substrate must be an electrical insulator because of the sensing element and the connections painted onto its surface. It should be a thermal insulator (low thermal diffusivity) in order to magnify the surface temperature increase, to maintain the semi-infinite assumption with a reasonable thickness and to minimize lateral conduction (1D hypothesis). Note that the 1D hypothesis requires that the gauge is located sufficiently far away from sharp edges and surface discontinuities.

Different types of thin-film gauges are used for turbomachinery applications. In stationary linear or annular cascade facilities, the entire blade can be machined out of ceramic, typically Macor because of its good machinability (Arts & al., 1990). The sensing element can be implemented at any desired location on the surface, and the substrate is sufficiently thick to ensure the semi-infinite assumption. Unfortunately, this technique is not usable for rotating blades because the ceramic would not withstand the centrifugal force. An alternative is to use inserts as shown in Figure 1.

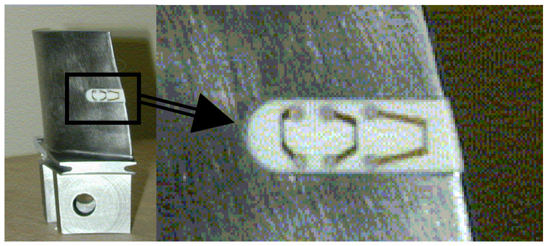

Figure 1: Macor insert fitted in a CT3 rotor blade

A cavity is grooved in the blade and the ceramic insert restitutes the blade shape. This technique has been applied to instrument the rotor blades of the CT3 turbine test rig at VKI (Dénos, 1996). However, the machining of the slots weakens the blade, especially in the case of internally cooled blades, and a stress analysis is required. A third technique consists in coating the metallic blade with vitreous enamel on which the film is painted. The difficulty of this technique lies in having a uniform coating thickness to avoid the calibration of each gauge (Hilditch & Ainsworth, 1990). Finally, a last option is to use thin-film painted on a thin polyamide sheet which is bonded on the blade surface thanks to a thin adhesive sheet. Guo & al., 1995, developed a sensor made of a platinum thin-film deposited on 50µm Upilex sheet.

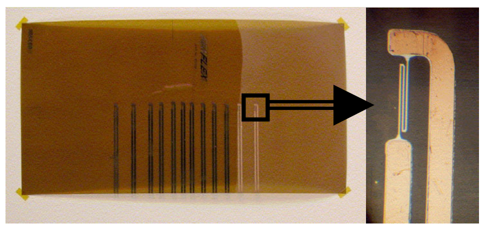

Figure 2: Two-layered substrate thin-film gauge

The commercial gauge used in this work consists of a 2.5mm serpentine nickel thin-film, with a resistance of 60Ω, painted on a 50µm thick Upilex-S sheet that can be glued on the blade surface with a 76µm thick double-sided adhesive sheet (Figure 2). Notice that the two last methods require a multi-layered data processing technique, as well as a specific calibration of the thermal properties for each layer. Unless necessary such as in the case of rotor blades, the use of highly conductive materials as a substrate should be avoided because the heat traverses quickly the instrumented sheet and enters the metal. Then, the semi-infinite hypothesis cannot be maintained for a long duration and the 1D hypothesis requires small curvatures.

The surface heat flux is derived from a measured surface temperature evolution. The 1D unsteady conduction equation for a multi-layered substrate system can be written as:

$$\frac{\partial^2 T(x,t)}{\partial x^2} = \frac{1}{\alpha(x)} \frac{\partial T(x,t)}{\partial t} \qquad (2)$$

where $\alpha = \frac{k}{\rho C}$, k being the thermal conductivity, ρ the density and C the specific heat.

The thermal properties are obviously depending on the considered location x inside the substrate. The solution of equation 2 provides the temperature profile inside the substrate at any time.

The necessary boundary conditions to solve this equation are:

- the surface temperature increase or the imposed heat flux,
- at the substrate interfaces $x=x_i$, the same value of heat flux and temperature for the two substrates:

$$-k_i \left(\frac{\partial T_i}{\partial x}\right)_{x=x_i} = -k_{i+1} \left(\frac{\partial T_{i+1}}{\partial x}\right)_{x=x_i} \quad i \leq n\text{-}1 \qquad (3)$$

and $T_i(x_i) = T_{i+1}(x_i)$ (4)

- at the backside of the substrate $x=L$, a known value of temperature T(L,t) (initial temperature in the case of semi-infinite assumption) or a known value of heat flux.

Then, the heat flux at the surface is computed thanks to the Fourier law:

$$\dot{q}_{wall\,1}(t) = -k_1 \left(\frac{\partial T_1}{\partial x}\right)_{x=0} \qquad (5)$$

Although α is used in equation 2 and k in equation 5, it can be shown that the value of the heat flux at the wall will depend only on $k/\sqrt{\alpha} = \sqrt{\rho C k}$, i.e. the so-called thermal product. For this reason, the accuracy on the heat flux is directly linked to the accuracy on the thermal product.

Schultz and Jones, 1973, propose a criteria for the thickness that is required to satisfy the semi-infinite assumption based on the constant heat flux solution for one layer. This thickness is defined as the one for which the ratio $\frac{\dot{q}(x)}{\dot{q}(x=0)} \leq 1\%$ i.e when $x = 3.648\sqrt{\alpha t}$. Characteristic values are shown in Table 1.

Material	α [10^6 m^2/s]	d [mm]
Upilex	0.17	1.5
Macor	0.88	3.4
Quartz	0.90	3.5
Steel	4.95	8.1

Table 1: Thermal diffusivity and thickness d required for semi-infinite assumption and a 1s duration step test for several materials.

ANALYTICAL SOLUTIONS

In the case of a single-layer thin-film gauge, the general solution of equation 2 can be obtained using the Laplace transform (Schultz & Jones, 1973). In the particular case of a step function in heat flux applied to the gauge, an analytical solution exists:

$$T_{wall}(t) - T_0 = \frac{2\,\dot{q}_{wall}}{\sqrt{\pi}} \frac{\sqrt{t}}{\sqrt{\rho C k}} \qquad (6)$$

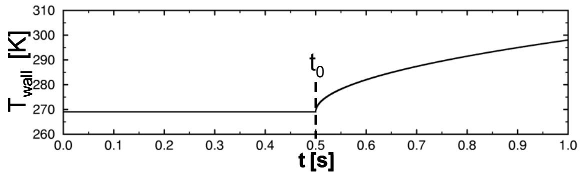

Figure 3 : Surface temperature evolution for single-layered substrate Macor gauge.

A typical surface temperature increase is shown in Figure 3 that was constructed mathematically for a single-layer Macor gauge. This evolution can be linearized when plotted as a function $\sqrt{t-t_0}$ as shown in Figure 4.

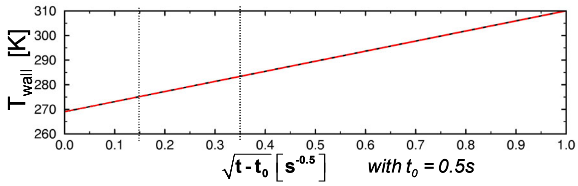

Figure 4 : Linearization of the surface temperature evolution for a single-layered substrate gauge

This can be very convenient to determine the thermal product $\sqrt{\rho C k}$ when a known heat flux is applied or vice-versa. However, the result of this linearization depends on the value of t_0, the time at which the surface temperature starts to rise. Experimentally, it is difficult to generate a step function and the time t_0 cannot always be determined with accuracy. For the case presented here, an error of only 0.01s on t_0 induces an error of 10% on the value of the heat flux computed with the slope (Figure 5) compared with the exact one ($\dot{q}_{wall} = 75250 W/m^2$) as obtained from Figure 4.

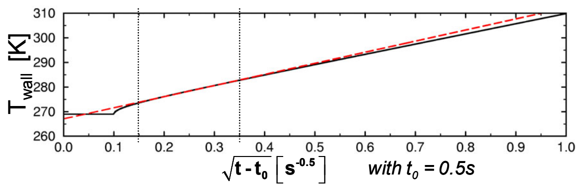

Figure 5 : Linearization of the surface temperature evolution with an error on the time t_0

There also exists an analytical solution for a step in fluid temperature and constant heat transfer coefficient h (Whitaker, 1976):

$$\frac{T_{wall}(t) - T_{wall}(t=0)}{T_{gas} - T_{wall}(t=0)} = 1 - e^{(\beta^2)}\,\mathrm{erfc}(\beta) \qquad (7)$$

with $\beta=\frac{h\sqrt{t}}{\sqrt{\rho C k}}$ (8)

The constant heat flux and constant temperature solutions are compared in Figure 6.

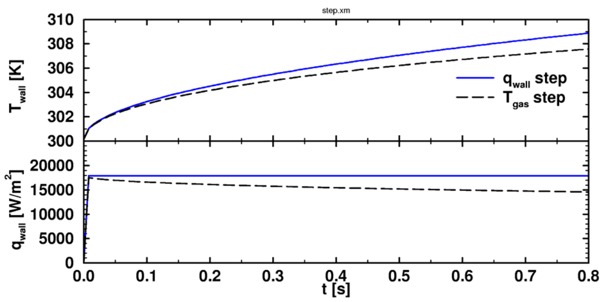

Figure 6: Analytical solutions: constant heat flux and constant temperature.

In the case of the two-layered substrate thin-film gauges, an analytical solution exists for the step in heat flux, Doorly & Oldfield, 1986:

$$T_{wall}(t)=\frac{2\,\dot{q}_{wall}}{\sqrt{\pi}\,\sqrt{\rho_2 C_2 k_2}}\sqrt{t}+\dot{q}_{wall}\frac{d_1}{k_1}\left[1-\frac{\rho_1 C_1 k_1}{\rho_2 C_2 k_2}\right] \quad (9)$$

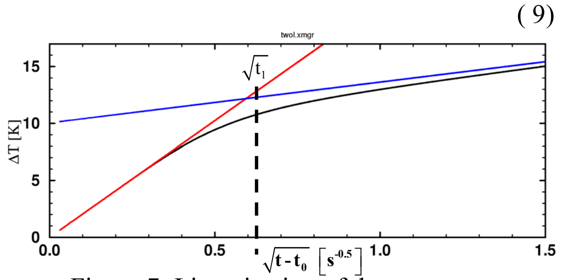

Figure 7: Linearization of the temperature evolution for a two-layered substrate thin-film gauge.

Similarly, the surface temperature increase can be plotted as a function of $\sqrt{t-t_0}$ (Figure 7) and the thermal products of the two successive layers are inversely proportional to the two successive slopes. In addition, the intersection between these two slopes, the "switch point", characterizes the thickness of the top layer. The so called thermal thickness parameter is defined as:

$$\frac{d_1}{k_1}=\sqrt{t_1}\,\frac{\frac{1}{\sqrt{\rho_1 C_1 k_1}}-\frac{1}{\sqrt{\rho_2 C_2 k_2}}}{1-\frac{\rho_1 C_1 k_1}{\rho_2 C_2 k_2}}\,\frac{2}{\sqrt{\pi}} \quad (10)$$

If the heat flux is known, the thermal properties can be derived and vice-versa. Here also, the knowledge of the time t_0 is important in order to avoid errors, especially on the determination of the first slope. Regarding the second slope, it will be reached only at large times. Very often, neither the area of the heat flux source nor the material thickness are sufficient to maintain the semi-infinite assumption or/and the 1D assumption for large durations. This means that the value of the second slope depends to a large extent on the two limits that have been selected to compute it.

Although the analytical solutions are very didactic and are often used to determine the thermal properties of substrates, there are not very useful for the data reduction of a real test. Analog circuits can be built that mimic the transfer function linking the surface temperature increase to the wall heat flux. Numerical solutions are more attractive and flexible.

NUMERICAL SOLUTION

As mentioned before, the wall heat flux is obtained by solving the 1D unsteady conduction equation in the successive substrates (equation 2) with temperature histories or heat flux histories at the surface and at a given depth as boundary conditions. The temperature history inside the substrate is then obtained and the wall heat flux is given by equation 5. The initial temperature distribution inside the substrate is assumed uniform because the substrate is under thermal equilibrium before the blow down.

The finite difference Crank–Nicholson scheme consists of an arithmetic average of the explicit and implicit formulation of the space derivative for equation 2:

$$\frac{T_j^{m+1}-T_j^m}{\Delta t}=\eta\left[\frac{\left(\frac{\alpha_j}{\Delta x_j}\left(T_{j+1}^{m+1}-T_j^{m+1}\right)\right)-\left(\frac{\alpha_{j-1}}{\Delta x_{j-1}}\left(T_j^{m+1}-T_{j-1}^{m+1}\right)\right)}{\frac{\Delta x_{j-1}}{2}+\frac{\Delta x_j}{2}}\right]+(1-\eta)\left[\frac{\left(\frac{\alpha_j}{\Delta x_j}\left(T_{j+1}^{m}-T_j^{m}\right)\right)-\left(\frac{\alpha_{j-1}}{\Delta x_{j-1}}\left(T_j^{m}-T_{j-1}^{m}\right)\right)}{\frac{\Delta x_{j-1}}{2}+\frac{\Delta x_j}{2}}\right] \quad (11)$$

where *j* is for the space step, *m* is for time. Notice that η is a numerical parameter that controls the stability of the scheme. This stability is ensured unconditionally if η is larger than 0.5, i.e. time step and space step are completely decoupled. If the unknowns at time $m+1$ are expressed as a function of the computed solution at time m, a tri–diagonal system is obtained that can be efficiently solved with existing algorithms. The solution provides the distribution of temperature in the gauge substrate at time step $m+1$.

The time step is obviously the sampling frequency. The space step can be variable but an accurate solution requires a minimum of smoothness in the value of the space step change. A clustering is applied close to the endwall where the strongest gradients are located and where the heat flux must be evaluated. Low–pass filtering is applied to avoid the large amplification of high frequencies that is inherent to the transfer function that links the surface temperature to the heat flux. Indeed, the solution of the conduction equation in the Laplace domain (Schultz and Jones, 1973) gives:

$$\overline{T}\left(x=0,p\right) = \frac{\overline{\dot{q}}}{\sqrt{\rho C k}\ \sqrt{p}} \qquad (12)$$

In the Fourier domain, *p* reduces to $j\omega$. This means that if one considers two sinusoidal heat flux variations of the same amplitude, one being at low frequency (e.g. 1 Hz) and the second at high frequency (e.g. 1 kHz), the last will produce a much lower surface temperature change than that at low frequency ($\sqrt{1000/1}=31.6$ times smaller). This also means that noise at high frequency on the sensor temperature signals will be greatly amplified on the reconstructed heat fluxes.

The data reduction program has been successfully validated versus test cases for which analytical solutions exist for one and two layers of substrate. In Figure 8, solutions of the surface temperature history are presented for one and two-layered substrate with a step in heat flux and a constant temperature in the backside of the substrate for boundary conditions. The comparison with analytical solution is very good.

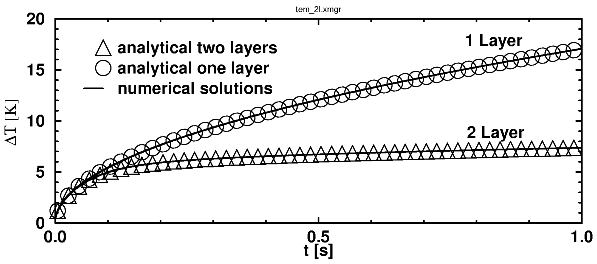

Figure 8: Agreement between analytical solutions for constant surface heat flux (*10800W/m*^{2}) and numerical computations of surface temperature with the Crank Nicholson scheme.

A more difficult test case is to impose the wall surface temperature described by the analytical solution to obtain a step in heat flux with the wanted magnitude. This is shown in Figure 9 for a two-layered substrate case.

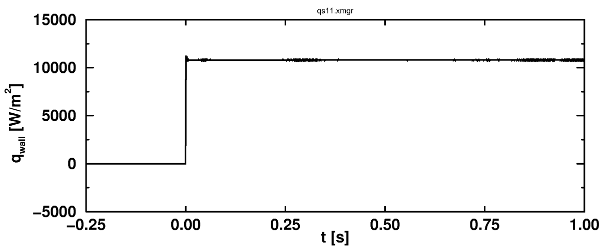

Figure 9: Calculated surface heat flux (10800W/m^2) with the Crank Nicholson scheme.

This data reduction technique can be used to compute the surface heat flux from the corresponding temperature history and vice-versa without any restrictive hypothesis on the boundary conditions.

THERMAL PRODUCT DETERMINATION

As mentioned previously, the uncertainty on the heat flux magnitude is directly proportional to the value of the thermal product $\sqrt{\rho C k}$. Very often, a difference is observed between the thermal properties given by the manufacturer for the bulk material and the values obtained by global determination of the thermal product. In addition, manufacturers never provide uncertainty bands and thus the overall uncertainty cannot be evaluated. Dénos, 1996, determined experimentally with the electrical discharge method a value of 2073 J/(m^{2}Ks$^{0.5}$) for Macor while the manufacturer provides a value of 1780 J/(m^{2}Ks$^{0.5}$). The difference is mainly attributed to the implementation of the sensing element that is fired at high temperature on the substrate. The high temperatures applied on an insulating material may affect its thermal properties, as mentioned by Schultz & Jones, 1973. In addition, the thermal thickness parameter must also be determined for the two-layered substrate gauge.

If a step function in heat flux of known amplitude is applied on the surface where the thin-film is painted, the temperature history allows determining the required parameters with equation 6 for a single-layer gauge and with equations 9 and 10 for a two-layered substrate gauge. A step in heat flux can be achieved by Joule heating: a step in current intensity is applied to the gauge (Dénos, 1996). In this case, only the gauge is heated and the 1D assumption is quickly ruined limiting the testing time to a few milliseconds. This cannot be used in multi-layered substrate system because only the top layer can be tested properly. In addition, the 'visible' area of the gauge cannot be used as such for the determination of the heat flux and tests under vacuum and a liquid of known thermal properties (e.g. glycerin) are required to eliminate this unknown. Thus, the thermal product relies on the thermal product of another material.

A second technique consists of a LASER as the heat source, as done by Thorpe & al., 2000. The advantage is that the beam covers a large area around the gauge, so that the 1D conduction assumption remains valid for longer durations. This method was also evaluated at VKI (Galván, 2001) but even if the power emitted by the laser is well known, it differs from the one received by the gauge because of reflection. Additionally, the reflection is different on the gauge and on the substrate.

Finally, it was decided to use a jet of hot air as a heat source similarly to Piccini & al., 2000.

Heat flux source characterization

The jet is heated at 340K and exits a 15mm diameter nozzle preceded by a settling chamber. In order to control the test conditions, the total pressure and temperature are measured inside the settling chamber of the nozzle. This temperature was used for the value of T_{gas} in the heat transfer coefficient computation (see equation 1). The step function applied to the gauge is obtained with a fast opening shutter placed between the gauge and the nozzle. Preliminary measurements of temperature, velocity, turbulence intensity and heat flux profiles for several distances from the end of the nozzle have been performed. At an axial distance of 15 mm downstream of the nozzle, the aero–thermal conditions are reasonably constant over 80% of the diameter. This ensures the 1D hypothesis over the test duration (typically less than 2s for a Macor substrate).

Then, the heat exchange coefficient was determined using a reference Macor gauge for which the thermal product was determined by electrical heating (2073 $J/(m^2Ks^{0.5})$). A number of gas temperature steps were applied to the gauge for various axial distances and jet velocities. The heat exchange coefficient was then computed using two different techniques.

The first method uses the analytical solution for a step function in gas temperature (equation 7). An optimisation procedure is used. It is based on the minimization of a function using a quasi-Newton algorithm from the mathematic library Nag. The routine finds the value of $h/\sqrt{\rho Ck}$ that provides the best fit of the experimental data. The thermal product being known, the heat exchange coefficient *h* results.

The second method consists in computing the surface heat flux evolution with the Crank-Nicholson scheme. Then, the heat transfer coefficient is obtained by averaging its instantaneous values calculated with equation 1.

The results are presented under the form of a Nusselt number (equation 13) as a function of a Reynolds number (equation 14).

$$Nu = \frac{h\,D}{k_{air}} \quad (13)$$

$$Re = \frac{U\,D}{\nu_{air}} \quad (14)$$

The results of both methods are plotted in Figure 10. In both cases, a very good test-to-test repeatability is achieved: less than 1%. The difference between the two methods is also below 1%.

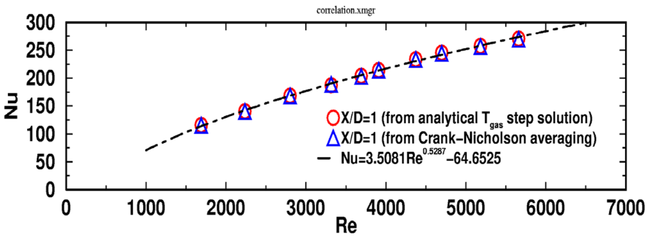

Figure 10 : Nusselt – Reynolds correlation obtained with single-layered substrate thin-film gauge

A Nusselt/Reynolds correlation is derived based on a power law:

$$Nu = 3.5081\ Re^{0.5287} - 64.6525 \quad (15)$$

This relationship will be used to determine the heat exchange coefficient *h* when calibrating other gauges.

Calibration using an analytical solution

The two-layered substrate thin film gauges were implemented on three types of substrates: Macor, quartz and steel. In the case of the Macor test piece, two layers of glue and Upilex were used. This intends to check if the glue layer can be distinguished from the Upilex as well as to enlarge the duration for which this assembly is tested. Similarly to Macor, quartz has `well known` thermal properties. The last gauge is in fact one of the gauge of the array that is implemented on the stator blade to be tested.

Steps in gas temperature were applied to the different samples. The correlation determined previously is used to provide the value of *h* depending on the velocity. In the case of two-layered substrate gauges, the only analytical solution available is, to the authors' knowledge, for a constant heat flux. For this reason, it was decided to use a superposition technique as described by Piccini & al., 2000 in order to correct the constant gas temperature experiment to a constant heat flux experiment. The technique consists in determining the transfer function that will transform the variable heat flux obtained during the constant gas temperature experiment (equation 16) into a constant heat flux (equation 17).

$$\dot{q}_{wall\,1}(t) = h\left(T_{gas} - T_{wall\,1}(t)\right) \quad (16)$$

$$\dot{q}_{wall\,2} = Cte \quad (17)$$

To apply a transfer function in the discrete time domain, a convolution is performed between the discrete heat flux and the discrete transfer function (a product in the frequency domain becomes a convolution in the time domain). At time $t=m\Delta t$, one has:

$$\sum_{i=0}^{m} a(m)\,\dot{q}_{wall\,1}(m-i) = \dot{q}_{wall\,2}(m) = Cte \quad (18)$$

where *a(m)* are the coefficients of the transfer function in the time domain. Equation 18 can be written for all successive time steps and solved to obtain the coefficient *a(m)* (see Piccini & al., 2000).

For both cases (constant heat flux or constant gas temperature), it is the same transfer function TF_1 that allows deriving the wall heat flux from the surface temperature i.e. the solution of the unsteady heat conduction equation. As a consequence, if a transfer TF_2 is applied to the heat flux $\dot{q}_{wall\,1}(t)$ in order to obtain a constant heat flux $\dot{q}_{wall\,2}$, this same transfer function TF_2 can be applied on the surface temperature $T_{wall\,1}$ to obtain $T_{wall\,2}$:

$$T_{wall\,2}(m) = \sum_{i=0}^{m} a(m)\, T_{wall\,1}(m-i) \qquad (19)$$

Figure 11 shows a temperature evolution measured with a single-layer Macor thin-film gauge as well as the signal corrected with the superposition technique. Figure 12 shows the corresponding heat fluxes computed with the Crank-Nicholson scheme as well as the analytical solution. This validates the technique applied to a one layer gauge but it can also be applied to a two-layered substrate gauge.

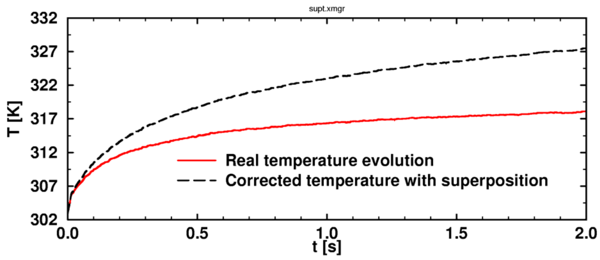

Figure 11 : Superposition technique : temperature correction

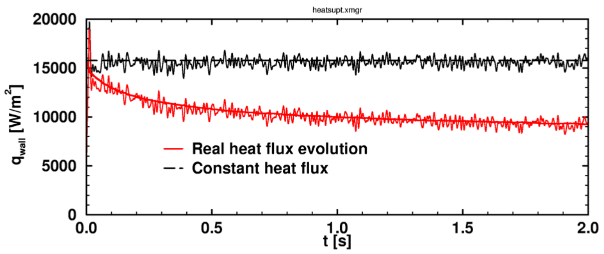

Figure 12 : Superposition technique : surface heat flux computation

Once the surface temperature measured by a two-layered thin-film gauge is corrected with the superposition technique, it is fitted with the analytical solution (equation 9) using the iterative optimization routine mentioned earlier. The optimization routine modifies at each iteration the two thermal products and the thermal thickness parameter and compares the analytical solution with the experimental data until a good fit is obtained (see Figure 13).

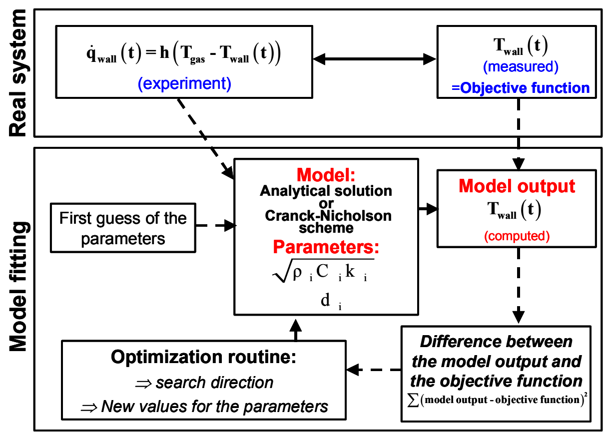

Figure 13 : Optimization algorithm principle

Note that in the case of the 2 layers of Upilex and glue on Macor, the analytical solution for a two-layered substrate fits very well. This means that the two successive sequences Upilex/glue can be considered as a unique one. In other words, the thermal properties of the glue are very close to the one of the Upilex.

The results are presented in Table 2. The manufacturer values are also reported as well as the test-to-test repeatability. Regarding the thickness, the value in between brackets is the one that was measured at the workshop after assembly. In general, all the values tend to be above the value of the manufacturer. The lowest dispersion on the value for Upilex is achieved with the Macor substrate, probably due to the two layers of Upilex and glue. The value for Macor is naturally quite close to the one determined with electrical heating (2073) that was used as a reference for the jet heat flux determination. The largest dispersions are observed for the sample on steel. In practice, even if the data reduction were performed with a value that is twice as much, the difference on the heat flux would not be large. In any case, this technique is much more accurate than the one based on the linearization because the fit is performed on the entire signal.

	$\sqrt{\rho C k}$ Upilex [J/m²Ks^0.5]	Upilex Thickness [µm]	$\sqrt{\rho C k}$ 2nd layer [J/m²Ks^0.5]
on Macor (8 tests)	747	310	2255
Dispersion (20:1)	2.1%	15.1%	6.1%
Manufacturer value	692	250 (350)	1780
on quartz (9 tests)	787	168	1763
Dispersion (20:1)	3.7%	5.2%	5.1%
Standard value	692	125 (150)	1521
on steel (5 tests)	732	177	10570
Dispersion (20:1)	13.4%	10.2%	20.6%
Standard value	692	125 (150)	8088

Table 2 : Results using the analytical solution

Calibration using the numerical solution

The procedure is very similar to that described in the previous section. The difference is due to the fact that it is not an analytical solution that is fitted but the result of the Crank-Nicholson scheme.

For each test, the heat flux history is derived from the *h* provided by the correlation (equation 15), the measured surface temperature increase and gas temperature:

$$\dot{q}_{wall}(t) = h\left(T_{gas} - T_{wall}(t)\right) \qquad (20)$$

This is compared with the heat flux computed from the measured surface temperature increase using the Crank-Nicholson scheme. The parameters (the two thermal products and the thickness) are varied until the computed heat flux history matches the experimental one.

The results obtained are presented in Table 3. Apart from the steel, the obtained thermal properties are very similar to the previous technique. The results are less scattered especially in the case of the steel substrate. The higher accuracy of this method is probably due to the fact that there is no need to compensate the temperature signal to a pseudo constant heat flux and the initial time of the step is not required. The gas temperature could even vary.

The thermal properties of the substrates being known and the data reduction technique for multi-layered substrate being available, measurements can now be performed.

	$\sqrt{\rho C k}$ Upilex [J/m²Ks$^{0.5}$]	Upilex Thickness [µm]	$\sqrt{\rho C k}$ 2nd layer [J/m²Ks$^{0.5}$]
on Macor (8 tests)	731	305	2117
Dispersion (20:1)	2.3%	3.9%	5.9%
Manufacturer value	692	250 (350)	1780
on quartz (9 tests)	752	167	1726
Dispersion (20:1)	3.9%	3.9%	4.9%
Manufacturer value	692	125 (150)	1521
on steel (5 tests)	699	175	8147
Dispersion (20:1)	8.8%	8.7%	9%
Manufacturer value	692	125 (150)	8088

Table 3 : Results using the numerical solution.

EXAMPLE OF MEASUREMENTS

In order to apply this measurement technique in a facility, a blade of the second stator of the CT3 turbine test rig has been instrumented with an array of 12 thin-film gauges (see Figure 14). The Upilex sheet covers the surface of the blade, and the sensing elements of the gauges are located around the leading edge, at mid-span of the blade height.

The VKI CT3 blowdown test rig allows a correct scaling of the Reynolds and Mach numbers but also of the temperature ratio T_{gas}/T_{wall} encountered in real gas turbine engine. During the 0.4 s duration test, the gas temperature changes almost like a step, the stator blade being initially at ambient temperature.

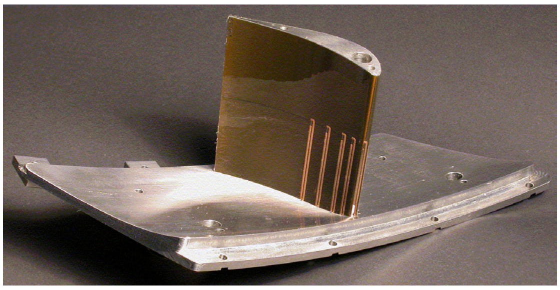

Figure 14 : Instrumented Upilex sheet implemented on the second stator measurement cassette

The gauges are connected to electronic boards equipped with a frequency compensation circuit. The fluctuations at high frequency are amplified according to the transfer function reported in equation 12. This allows improving the resolution of the rotor blade passing events recorded on the 12 bit data acquisition system.

The time-averaged component of the signal is low pass filtered at 750 Hz and sampled at 1.5 kHz. The time-resolved component is high-pass filtered at 100 Hz and sampled at 300 kHz.

The surface temperature history of each gauge is converted into heat flux (see Figure 15) using the Crank Nicholson scheme and the thermal properties: $\sqrt{\rho C k}_{Upilex} = 699 J/m^2 K^{0.5}$, d_{upilex}=175 µm and $\sqrt{\rho C k}_{Steel} = 8147 J/m^2 K^{0.5}$.

The heat flux is averaged over a portion of ~0.1s over which the operating conditions stay reasonably constants.

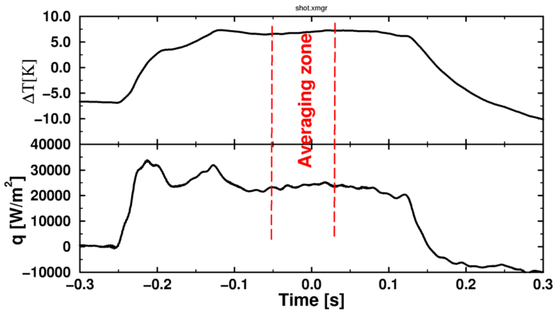

Figure 15 : Temperature history and computed heat flux history for gauge

Finally, the heat transfer coefficient *h* is computed with equation 1 and the Nusselt number based on the blade chord can be derived from:

$$N_u = \frac{\dot{q}\, c}{k_{gas}\left(T_{gas} - T_{wall}\right)} = \frac{h\, c}{k_{gas}} \qquad (21)$$

The Nusselt number distribution is shown in Figure 16. The values obtained at the leading edge are unrealistic probably because the 1D assumption is probably not satisfied in this region of high curvature. The ratio of the exposed surface to the thermal inertia is much smaller than that for a flat plate. It is likely that the surface temperature rise in the leading edge region is higher than that on a flat plate when imposing the same heat flux.

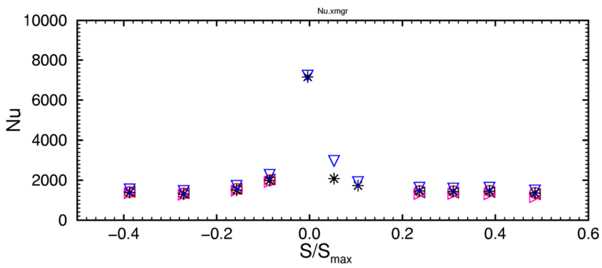

Figure 16 : Nusselt number distributions: repeatability

Finally, the unsteady part of the measurement is processed also with the Crank-Nicholson scheme. A phase-locked averaging routine provides an average period using 192 rotor passing events i.e. three rotor revolutions. On Figure 17 the phase-locked average of two identical tests is displayed showing the good repeatability of the measurements.

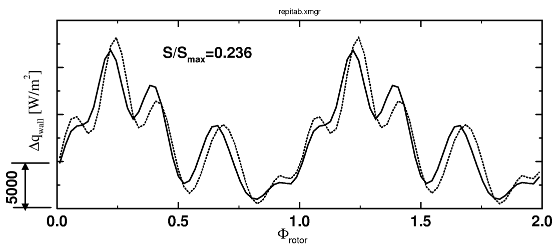

Figure 17 : PLA repeatability

CONCLUSIONS

A novel numerical data reduction technique that solves the unsteady 1D conduction equation using a Crank Nicholson scheme was developed and validated. It can handle multi-layered substrates and can use heat fluxes or surface temperatures as boundary conditions. Apart from the 1D hypothesis, there is no particular restriction.

In order to determine the thermal products of substrates, a jet was used as a heat flux source. It provides uniform heat flux over a sufficiently large area for the selected testing duration. The magnitude of the heat flux was assessed thanks to a reference gauge. The fact that this magnitude always relies on the thermal product of a material for which the thermal properties are supposed to be known is not satisfactory. The later use of test gauges on Macor or Quartz intended to have at least two reference materials.

Regarding the determination of thermal products, this was previously done using the lineralization of the analytical solution for constant heat flux. The accuracy of this method depends on the ability to generate experimentally a perfect step in heat flux and on the accurate knowledge of the time t_0 at which the step starts. In addition, it is easier to impose a step in gas temperature than in heat flux.

A first improvement is obtained by fitting analytical solutions using an optimization procedure. This can be done with both constant temperature and constant heat flux analytical solutions. In the last case, the constant temperature test can be converted to a virtual constant heat flux test using a superposition technique. The method is particularly powerful for two-layered substrates because it is difficult to maintain the 1D hypothesis for durations that are sufficiently long to determine accurately the thermal product of the second layer.

A second improvement consists in using the heat flux history and computing the wall surface temperature with the numerical scheme. The optimizer adjusts then the thermal properties (and thickness in the case of two-layered substrates) in order to match the measured surface temperature. This method does not require any particular hypothesis on the type of test, is not sensitive to the time t_0 in the case of step test and can be applied with multi-layered substrates.

Finally, the numerical data reduction technique and the determined thermal products were used to perform measurements on a stator blade with a thin-film array based on a Upilex substrate as a first layer and steel as a second layer. The results are reasonable away from the leading edge where the authors suspect that the 1D hypothesis is not satisfied. The time-resolved component (rotor blade passing events) was also obtained.

REFERENCES

Arts T., Lambert de Rouvroit M., and Rutherford A.W., 1990, '*Aero-thermal investigation of a highly loaded transonic linear turbine guide vane cascade (A test case for inviscid and viscous flow computations).'*, VKI TN 174.

Dénos R., 1996, '*Etude aérodynamique et thermique de l'écoulement instationnaire dans un rotor de turbine transsonique.'*, Ph.D. Thesis, Ecole Supérieur d'Ingénieurs de Poitiers.

Doorly J.E., and Oldfield M.L.G., 1986, '*New heat transfer gages for use on multilayered substrates.'*, Journal of Turbomachinery, Vol.108, pp 153-160.

Galván I., 2001, '*Assessment on the use of a LASER to determine the thermal product of thin-film gauge substrates.'*, VKI PR 2001-11.

Guo S.M., Spencer M.C., Lock G.D., Jones T.V., and Harvey N.W., 1995, '*Application of Thin-Film Gauges on Flexible Plastic Substrates to the Gas Turbine Situation.'*, ASME paper 95GT357.

Hilditch M.A., and Ainsworth R.W., 1990, '*Unsteady heat transfer measurements on a rotating turbine blade.'*, ASME paper 90GT175.

Piccini E., Guo S.M., and Jones T.V., 2000, '*The development of a new direct-heat-flux gauge for heat-transfer facilities.'*, Journal of Measurement Science and Technology, Vol.11, pp 342-349.

Schultz D.L., and Jones T.V., 1973, '*Heat transfer measurements in short duration hypersonic facilities.'*, AGARDograph Report 165.

Thorpe S., Yoshhino S., and Ainsworth R., 2000, '*Fabrication and calibration techniques for turbine rotor tip heat transfer gauges.'*, Proceeding of the 15th Symposium on Measuring Techniques for Transonic and Supersonic Flows in Cascades and Turbomachines, Florence.

Whitaker S., 1976, '*Elementary of heat transfer analysis.'*, Pergamon unified engineering series, Rober Maxwell.